IEEE Access
Multidisciplinary | Rapid Review | Open Access Journal

SPECIAL SECTION ON ADVANCED OPTICAL IMAGING FOR EXTREME ENVIRONMENTS

Received January 22, 2019, accepted February 8, 2019, date of publication February 15, 2019, date of current version March 7, 2019.

Digital Object Identifier 10.1109/ACCESS.2019.2899669

Comparative Study of TSM Scattering Characteristics Based on Improved Wen's Spectrum and Semi-Empirical Models

GENGKUN WU, JIANCONG FAN, FUXIN ZHANG, AND TING WANG

College of Computer Science and Engineering, Shandong University of Science and Technology, Qingdao 266590, China

Corresponding author: Gengkun Wu (wugengkun@sdust.edu.cn)

This work was supported in part by the Shandong Provincial Natural Science Foundation under Grant ZR2018BD029, in part by the Scientific Research Foundation of Shandong University of Science and Technology for Recruited Talents under Grant 2017RCJJ046, in part by the Shandong Provincial Natural Science Foundation of China under Grant ZR2018MF009, the Special Funds of Taishan Scholars Construction Project, and Leading Talent Project of Shandong University of Science and Technology, in part by the National Key Research and Development Plan under Grant 2018YFC0831002, in part by the Scientific Research Foundation of the Shandong University of Science and Technology for Recruited Talents under Grant 2017RCJJ044, in part by the Natural Science Foundation of Shandong province under grant ZR2018MF001, and in part by the Project of Shandong Province Higher Educational Science and Technology Program under Grant J17KA076.

ABSTRACT Combining the contrast characteristics of Wen's directional spectrum and Donelan's distribution function, this paper proposed a simulation model of 2-D random rough sea surface based on improved Wen's spectrum and Monte Carlo method, and analyzes distribution characteristics of the 2-D random rough sea surface under the condition of 320° wind direction, different wind speeds, and fetch. On the basis of the classical two-scale method for calculating the electromagnetic scattering of the sea surface, this paper attempts to compare the electromagnetic scattering results of the above simulated 2-D random rough sea surface with the backscattering simulation data of four typical semi-empirical sea clutter models, such as Technology Service Corporation, the Georgia Institutes of Technology, the Hybrid Sea Clutter Model, and the Naval Research Laboratory for the first time. Then, the electromagnetic scattering characteristics of 2-D random rough sea surface with improved Wen's spectrum in HH and VV polarization modes under different sea conditions, grazing angle, and incident frequency are studied. Finally, this paper analyzes the fitting characteristics between the above model and improved Wen's spectrum from the perspective of inversion of the wave spectrum by combining the spectral characteristics of the simulated wave spectrum and summarizes the respective adaptive ranges of different models.

INDEX TERMS Donelan's distribution function, improved Wen's spectrum, Monte Carlo method, two-scale method, semi-empirical sea clutter models.

I. INTRODUCTION

As a hot topic on ocean remote sensing, the electromagnetic scattering of two-dimensional random rough sea surface has aroused the widespread concern of scholars both at home and abroad. Regarding sea clutter, it generally refers to the backscattering of sea surface under radar illumination [1], [2]. The radar's working mode is the detection of echo signals with radiated electromagnetic energy. In this process, the existence of clutter interference has an inevitable impact on the detection and tracking of sea surface target, thereby reducing the performance of radar system. As a result, the detection effect of radar in the marine environment is mainly improved by the suppression of sea clutter. Calculating the backscattering coefficient by simulating the sea surface is the main method of simulating sea clutter in recent years. During the course of exploring the reconstruction of sea surface, two important methods including fractal-like function method and the classical Monte Carlo method applied to the simulation of random rough sea surface have been developed [3], [4].

The associate editor coordinating the review of this manuscript and approving it for publication was Huimin Lu.

As one of the most classical methods among the electromagnetic scattering approximation methods of calculating random rough sea surface, the two-scale method effectively improves computational efficiency by means of physical approximation [5].

In actual research, it is found that sea clutter is affected by a number of factors, mainly including natural factors and radar parameters [6]. Mainly applied to study the mean value change of sea clutter scattering coefficients with the change of grazing angle and marine environmental parameters, the mean scattering coefficient model of sea clutter plays an important role in predicting the distance performance of radar under the background of sea clutter. A series of sea clutter measurements have been conducted by the US Naval Research Laboratory for nearly two decades. The airborne 4-frequency radar (4FR radar) used by the researchers of its experiments was distributed in the UHF band (428MHz), L-band (1228MHz), C-band (4455MHz) and X-band (8910MHz). In the case of 5∼50km/h wind speed and 5°∼90° grazing angle, horizontal and vertical polarization methods were adopted by researchers to measure the sea clutters under downwind, upwind and crosswind conditions respectively [6]. Standard metal balls were used by the method for the purpose of calibrating hardware. In addition, the measurement ship was innovatively used to keep a record of the observed sea area's wind speed and wave height. Some airborne measurements were recorded by Masuko in his work, and the early data was summarized by later books on radar systems compiled by Skolnik and Nathanson. Subsequently, marine satellites and SIR-A were launched by the United States to SIR-C spacecraft-borne radars. Performing two flight missions, the SIR-C was equipped with L, C and X-band multi-polarization imaging radars. The earth was mapped by the radar to obtain the scattering coefficient of the ground surface. So far, radar satellites have been launched by the ESA and countries such as Russia, Japan and Canada to obtain a large amount of scattering data on ground and sea surface. Some semi-empirical sea clutter mean scattering coefficient models are derived by many scholars from the measured sea clutter data to supplement the scattering coefficients without being measured by the experiment [7]. Known as the GIT model, a sea clutter mean scattering coefficient model was derived by the researchers from the Georgia Institutes of Technology.

Different from traditional sea clutter-based simulation models, radar parameters and environmental factors are used to simulate and suppress sea clutter. Based on the theoretical power spectrum of the Wen's spectrum and the experimental results of the Donelan's distribution function [7], the two-dimensional random rough sea surface model is simulated by the Monte Carlo method in this paper. On the basis of the model, electromagnetic scattering coefficient is calculated by classical TSM method [5] and compared with the backscattering simulation data of four typical sea clutter semi-empirical models including Technology Service Corporation, Georgia Institutes of Technology, Hybrid Sea Clutter Model and Naval Research Laboratory models [8]. Finally, this paper analyzes the above experimental conclusions, and summarizes the adaptability of all models under different sea conditions, incident frequencies, grazing angles and wind speeds [9], [10].

Below is the structure of this paper. In part II, a description is given to the basic theory of the Monte Carlo method for the modeling of sea surface and the TSM method for the calculation of scattering coefficient. In part III, the Monte Carlo method combined with the Wen's power spectrum and the Donelan's direction distribution function is used to simulate the two-dimensional random rough sea surface, and studies are carried out on the wave distribution characteristics of the simulated sea surface under different sea conditions. Based on the simulation results above, studies are conducted on the electromagnetic scattering characteristics of two-dimensional sea surface simulated by improved Wen's spectrum, and an analysis is conducted on the fitting characteristics of semi-empirical models and improved Wen's spectrum by comparing the electromagnetic scattering calculation results of the above simulated two-dimensional random rough sea surface with the backscattering simulation data of four typical sea clutter semi-empirical models including GIT, TSC, HYB and NRL models. In this part, we extract the two-dimensional simulation spectrum of different wind speeds in the fixed wind zone and 320° direction along the spectral direction of the semi-empirical model, and then calculate the backscattering coefficient based on the two-scale method. Finally, a discussion is held on recent work and a summary of this paper is made in part IV.

II. PRELIMINARY

A. TWO-DIMENSIONAL RANDOM ROUGH SEA SURFACE MODELING BASED ON MONTE CARLO METHOD OF IMPROVED WEN'S SPECTRUM

In the exploration of sea surface reconstruction, the Monte Carlo method [11] is a classical method for the simulation of random rough sea surface. Its basic idea is to filter the one-dimensional power spectrum function in the frequency domain, perform inverse fast Fourier transform based on this operation, obtain the height fluctuation of the random rough sea surface, and finally simulate the random rough sea surface. The amplitude of harmonics is an independent Gaussian random variable whose variance is proportional to the power spectrum $S(k_j)$ of a specific wave number since the rough surface is considered to be a superposition of numerous harmonics. Therefore, length L's one-dimensional random rough surface sample can be generated by the following function [12]:

$$f(x_n) = \frac{1}{L} \sum_{j=-\frac{N}{2}+1}^{N/2} F(k_j) e^{i \cdot k_j x_n} \tag{1}$$

wherein, $x_n = n\Delta x (n = -\frac{N}{2}+1, \ldots, N/2)$ represents the n^{th} sample point on the rough surface; $F(k_j)$ and $f(x_n)$ are called

Fourier transform pairs and defined as:

$$F\left(k_j\right)=\frac{2\pi}{\sqrt{2\Delta k}}\sqrt{S(k_j)} \cdot\begin{cases}[N(0,1)+iN(0,1)], & j=-\dfrac{\mathrm{N}}{2}+1,\ldots,-1\\ N\ (0,1), & j=0,N/2\end{cases} \tag{2}$$

wherein, $k_j = 2\pi j/\mathrm{L}$ is the expression giving a definition of the discrete wave number k_j; Δk stands for the spatial wavenumber difference of the harmonic samples adjacent to the spectral domain; $S(k_j)$ refers to the power spectral density of the rough surface; $N\ (0,\ 1)$ represents a random number of a normal distribution with a mean of 0 and a variance of 1. When $j > 0$, $F(k_j)$ satisfies the conjugate symmetry relationship $F(k_j) = F(k_{-j})^*$. In this case, the contour $f(x_n)$ of the rough surface obtained after Fourier inverse transform is guaranteed to be a real number.

The formula of the Wen's spectrum [13] is as follows:

$$\mathrm{S}\left(\sigma\right) = \frac{m_0}{\sigma_0}p\times\exp[-95\times(\frac{\sigma}{\sigma_0}-1)^{\frac{12}{5}} \times(ln\frac{p\left(5.813-5.137\eta\right)}{\left(6.77–1.088p+0.013p^2\right)\left(1.307–1.426\eta\right)})] \quad 0\le\frac{\sigma}{\sigma_0}\le 1.15 \tag{3}$$

$$\mathrm{S}\left(\sigma\right) = \frac{m_0}{\sigma_0}\times(1.15\frac{\sigma}{\sigma_0})^m \times\frac{6.77-1.088p+0.013p^2\left(1.307-1.426\eta\right)}{5.813-5.137\eta} \quad \frac{\sigma}{\sigma_0}\ge 1.15 \tag{4}$$

wherein, σ_0 is peak frequency; m_0 means zero moment; $P = \frac{\sigma_0}{m_0}s(\sigma_0)$ refers to spectral tip factor; $\eta = H''$, $m = 2(2-\eta)$ represents depth parameter; h stands for water depth; $\overline{H}$ means average wave height. On this basis, the relationship between m_0, σ_0, P and wind zone x, wind speed U and wind time t is established.

In the process of two-dimensional sea surface simulation, it is necessary to introduce an angle distribution function for correction, thereby reflecting the anisotropy exhibited by the sea spectrum resulting from wind direction. The directional spectrum is defined as the product of the direction function $G(\phi)$ and the spectrum $S(f)$: $S\left(f,\phi\right) = S(f)G(\phi)$. Wherein, the directional spectrum is $\begin{cases} S\left(f,\phi\right)=S(f)G(\phi)\\ \int_{-\pi}^{\pi}G(f,\phi)d\phi=1.\end{cases}$ In view of the fact that the Wen's directional spectrum shows worse effect of fitting with the measured data than the Donelan's distribution [14], and experimental verification has been conducted, the Donelan's direction distribution function obtained by the direct analysis of the Fourier transform method is used as the direction function. The expression is as follows:

$$\begin{cases} G\left(f,\theta\right)=\dfrac{1}{2}\beta sech^2\beta\theta\\ \beta=2.61(f/f_p)^{1.3}\ 0.65\le f/f_p\le 0.95\\ \beta=2.28(f/f_p)^{-1.3}\ 0.95<f/f_p\le 1.6\\ \beta=1.24\ f/f_p<0.65\ or\ 1.6<f/f_p\end{cases} \tag{5}$$

Given the fact that the deep water wind spectrum is more commonly used classical JONSWAP spectrum limited by the growth state of ocean waves itself, the above method is adopted in this experiment to model ocean waves based on the improved Wen's spectrum.

B. CALCULATION MODEL OF BACKSCATTERING COEFFICIENT FOR TWO-DIMENSIONAL RANDOM ROUGH SEA SURFACE

Two important methods including analytical approximation methods and numerical simulation methods have been developed to study electromagnetic scattering calculations on random rough sea surface. In this paper, the TSR method developed on the Kirchhoff approximation method adapted to large rough size and the SPM method adapted to small rough size are adopted, namely the two-scale method. In order to take the tilt effect of the rough surface into consideration, a method of averaging operation is adopted by the TSM method on a large-scale slope distribution [15], [16]. In the two-scale model, the backscattering coefficient is calculated as follows when the incident surface is in the x-z plane [17]:

$$\begin{cases} \theta^0_{HH}\left(\theta_i\right)=\int_{-\infty}^{\infty}\int_{-ctg\theta_i}^{\infty}(\hat{h}\cdot\hat{h}')^4\sigma_{HH}(\theta_i') \times(1+z_x tg\theta_i)P(z_x,z_y)dz_x dz_y\\ \theta^0_{VV}\left(\theta_i\right)=\int_{-\infty}^{\infty}\int_{-ctg\theta_i}^{\infty}(\hat{v}\cdot\hat{v}')^4\sigma_{VV}(\theta_i') \times(1+z_x tg\theta_i)P(z_x,z_y)dz_x dz_y\end{cases} \tag{6}$$

In the above formula, $\theta^0_{HH}\left(\theta_i\right)$ and $\theta^0_{VV}\left(\theta_i\right)$ represent the backscattering coefficients under different polarization states. The former subscript indicates the receiving polarization while the latter one stands for the transmitting polarization. z_x and z_y stand for the rough surfaces in the x and y directions respectively. θ_i and $\theta_i^{'}$ represent incident angle and local incident angle respectively. $\hat{h}'$, $\hat{h}'$, $\hat{v}$ and $\hat{v}'$ refer to the unit horizontal and vertical polarization vectors in reference and local coordinate systems respectively, Wherein, $P(z_x, z_y)$ means the large-scale roughness in the x and y directions. The scattering field can be solved by the KA approximation method under the premise of satisfying the approximation condition of the application KA since the incident wavelength is fixed and the large-scale part of the TSM model is constituted by the part of the spatial wavenumber in the rough surface $K \le K_L$. In the meanwhile, the small-scale part of the TSM model is composed of the part of the spatial wavenumber in the rough surface $K \ge K_S$, and the scattering

field can be solved by the SPM method. Certainly, the precondition is also the satisfaction of the first-order surrounding approximation. Besides, the spatial wave number $K = K_B = 2k_i sin\theta_i$ satisfying the Bragg scattering condition should also be contained in the small-scale portion of the rough surface. $\frac{1}{\sqrt[K]{\int_0^L \int_0^{2\pi} K^4 S(K,\Theta) dk d\Theta}} \geq \lambda$ is the judgment condition that should be satisfied in the case of determining the large-scale cutoff wave number K_L. $k_i \sigma_{small} cos\theta_i \leq 1$, $K_S < K_B = 2k_i sin\theta_i$ should be satisfied in the case of solving the small-scale part of the rough surface scattering cross section. In the above formula, $\sigma^2_{small} = \int_{K_S}^{+\infty} \int_0^{2\pi} S(K, \Theta) dk d\Theta$ represents the height undulating square root of the small-scale part, and k_i stands for incident spatial wave number. Then, K_S can be obtained.

III. RELATED WORK

A. TWO-DIMENSIONAL SEA SURFACE MODELING EXPERIMENT

Similar to the method of simulating the one-dimensional random rough surface by the above-mentioned Monte Carlo method, it is assumed that the lengths of the random rough surface to be generated in the x and y directions are L_x and L_y, the numbers of equally spaced discrete points are M and N, and the spacings between adjacent two points are Δx and Δy. Then, $L_x \approx M\Delta x$ and $L_y \approx N\Delta y$. As seen above, the height at each point $(x_m = m\Delta x, y_n = n\Delta y)(m = -\frac{M}{2} + 1, \ldots, \frac{M}{2}; n = -\frac{N}{2} + 1, \ldots, N/2)$ on the rough surface can be expressed as:

$$f(x_m, y_n) = \frac{1}{L_x L_y} \sum_{m_k=-\frac{M}{2}+1}^{M/2} \sum_{n_k=-\frac{N}{2}+1}^{N/2} F(k_{m_k}, k_{n_k}) \times \exp[i(k_{m_k} x_m + k_{n_k} y_n)] \quad (7)$$

wherein,

$$F\left(k_{m_k}, k_{n_k}\right) = 2\pi [L_x L_y S(k_{m_k}, k_{n_k})]^{1/2} \times \begin{cases} \frac{[N(0,1) + iN(0,1)]}{\sqrt{2}}, & m_k \neq 0, \frac{M}{2} \text{ and } n_k \neq 0, \frac{N}{2}; \\ N(0,1), & m_k = 0, \frac{M}{2} \text{ or } n_k = 0, \frac{N}{2}; \end{cases} \quad (8)$$

Similarly, $S(k_x, k_y)$ represents the power spectral density of a two-dimensional random rough surface, and $k_{m_k} = 2\pi m_k / L_x$, $k_{n_k} = 2\pi n_k / L_y$. Like the Monte Carlo modeling method in the one-dimensional rough surface, the Fourier coefficient must satisfy the following condition $F\left(k_{m_k}, k_{n_k}\right) = F^*(-k_{m_k}, -k_{n_k})$, $F\left(k_{m_k}, -k_{n_k}\right) = F^*(-k_{m_k}, k_{n_k})$ in order for $f(x_m, y_n)$ to be a real number.

Simulation is conducted for the two-dimensional random rough sea surface of the Wen's power spectrum and the Donelan's direction function through a combination of the fast Fourier transform and the above two-dimensional Monte Carlo simulation method. The simulation of the two-dimensional sea surface is based on the wave power spectrum, which only represents the distribution probability of the wave height energy with the position, and the three-dimensional random rough sea surface close to the real sea surface must consider the direction function. That is, $S(f, \phi) = S(f)G(\phi)$. Knowing the preconditions, the random phase θ must be distributed between $-\pi$ and π, and after adding the initial phase of the Wen's power spectrum, it is required to be distributed in the third and fourth quadrants in order to obtain the cosine function and the amplitude of the wave. It is positive. Therefore, the four-quadrant synthesis method is adopted, that is, the values of the first and second quadrants are accumulated by π, and the average distribution of the formulas (1) and (2) is applied to obtain an initial phase within a certain range, thereby achieving the requirement of random characteristics in a certain quadrant. Substituting the known condition $\begin{cases} S(f, \phi) = S(f)G(\phi) \\ \int_{-\pi}^{\pi} G(f, \phi) d\phi = 1 \end{cases}$ into formula (3) and (4). $x_n = n\Delta x (n = -\frac{N}{2} + 1, \ldots, N/2)$ represents the nth sample point on the rough surface, and the variation range is 1000m. F(k_j) and $f(x_n)$ are called Fourier transform pairs. In the actual simulation process, we take the two-dimensional Gaussian rough surface model with the relevant length $L_x = L_y$, which are 0.5λ, 1.0λ and 1.5λ respectively, where the root mean square height is $\phi = 0.1\lambda$, the x direction and the y direction length $L_x = L_y = 8.0\lambda$, 80 points per wavelength, multiplied by 10 wind zone, falling within 1000m. It can be found that the correlation length represents the period of change of the rough surface under the same rms condition. The smaller the correlation length, the more frequent the rough surface changes, and the smaller the direct distance between the peak and the peak. The results are presented in Fig.1$\sim$4, among which the above experimental data refers to the sea state parameter of the 320# data measured by the IPIX radar in 1993. Wind direction is selected to be 320°, humidity 81% and temperature 4.3°C. During the experiment, the two sets of experimental data under the two-level and three-level sea conditions are selected. Under the same sea conditions, the main wave wavelength positions of the sea spectrum model are consistent, and are roughly distributed around (0.05$\sim$0.06) rad/m. The wind speed at a height of 10 meters from the sea surface is the wind speed of the waves. In addition, the simulation results of the two-dimensional rough sea surface based on the improved Wen's spectrum are as follows:

By comparing Fig.1 with Fig.2 and Fig.3, it can be seen that the sea surface undulation (effective wave height) is greater with the increase of wind speed under the condition of constant wind direction and area and sufficient wind duration. Gravity wave sees larger undulations and tension wave experiences slow changes. More obvious distinction is discovered between large-scale gravity waves and small-scale tension waves. The above characteristics are in line with the natural variation of the ocean wave affected by external factors, especially wind speed. When the wind speed is small, the sea surface sees rapid local variation but small overall undulation. When the wind speed increases, the sea

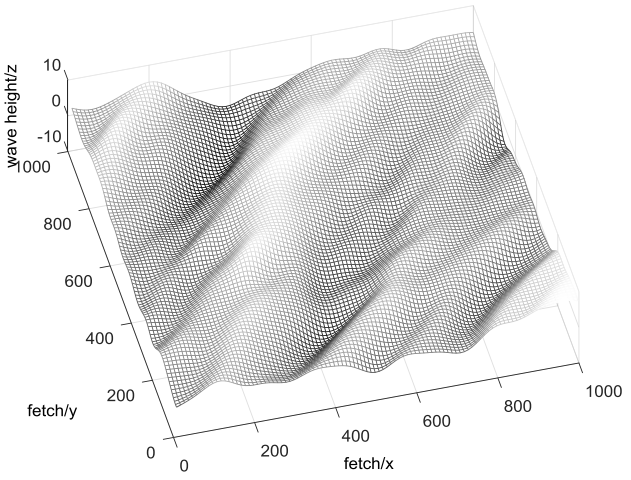

FIGURE 1. Simulated sea surface with a wind speed of 10km/h, a wind direction of 320° and a fetch of 10km.

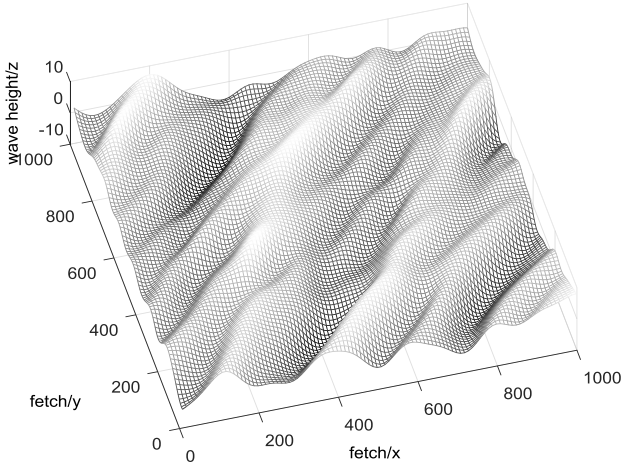

FIGURE 2. Simulated sea surface with a wind speed of 15km/h, a wind direction of 320° and a fetch of 10km.

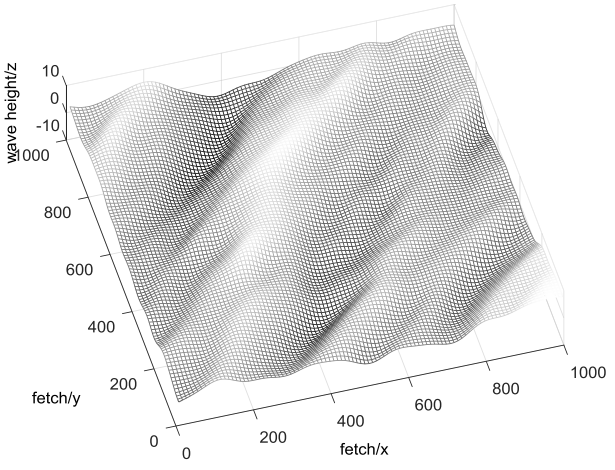

FIGURE 3. Simulated sea surface with a wind speed of 20km/h, a wind direction of 320° and a fetch of 10km.

surface sees an increase in overall undulation with slow local variation, showing consistency with the natural variation of ocean waves. From a qualitative point of view, the sea surface is repeatedly superimposed with ripples, bubbles and splashes on large-scale, near-periodic waves. It can be seen from the comparison test that the above simulation method can not only qualitatively simulate the large-scale wave into a skeletonized basic structure, but also express the fine superimposed body such as small-scale corrugation. This also lays the foundation for calculating the backscattering coefficient of random rough sea surface in the later part of this paper. That is, we can calculate the large-scale wave by the Kirchhoff approximation method, and then use the perturbation method to perform the quadratic ensemble operation on the large-scale scattering result, and finally realize the double-scale algorithm of the sea surface backscattering coefficient. This method is practical both in terms of simulation technology and wave distribution law.

By comparing Fig.3 with Fig.4, it can be seen that the sea surface sees a rise in undulation (effective wave height) with the increase of wind area. As displayed from Fig.4, the sea surface verges on a fully grown state in a sufficiently long wind zone, which clearly shows the influence of wind speed and zone on the growth state of waves and the roughness of sea surface. When the wind direction is 320°, waves are the same in undulations and movement directions, also according with physical ocean meaning. This fully proves that the wind zone is the same as the wind speed, and it also plays a direct role in the distribution of the wave roughness scale.

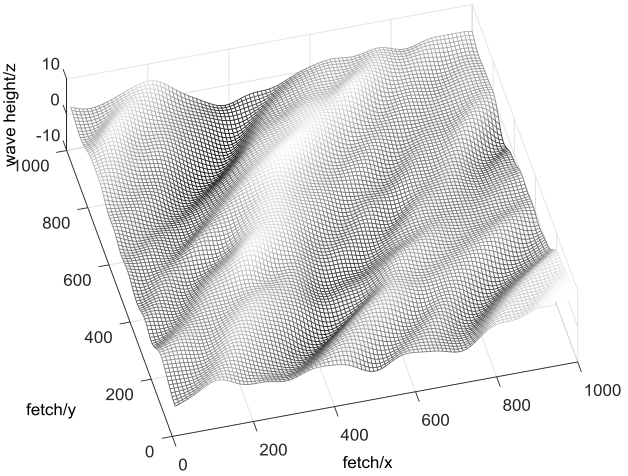

FIGURE 4. Simulated sea surface with a wind speed of 15km/h, a wind direction of 320° and a fetch of 20km.

B. COMPARISON EXPERIMENT BETWEEN TWO-SCALE METHOD AND SEA CLUTTER SEMI-EMPIRICAL MODEL

The intensity of sea clutter is represented by the radar cross-sectional area σ^0 per unit area. Typical semi-empirical models of sea clutter backscattering coefficients are GIT, HYB, TSC and NRL models, among which the GIT model is a backscatter coefficient model based on measured data and mathematical models of different sea surface scattering mechanisms. The parameters σ^0 in the model are associated with three factors, including interference factor, wind speed

factor as well as wind direction factor. The distinguishing feature of the GIT model lies in the simulation of sea surface with both wind speed and average wave height. In the case of fully developed sea surface, wind speed is correlated with average wave height. In the changing sea environment, wind speed and average wave height can be introduced as independent parameters. Below is the definition of the GIT model [8]:

When the transmission frequency of the radar varies from 1GHz to 10GHz,

$$\sigma^0_{HH} = 10\log(3.9\times10^{-6}\lambda\theta^{0.4}F_aF_uF_w) \tag{9}$$

$$\sigma^0_{VV} = \begin{cases} \sigma^0_{HH} - 1.05\ln(h_a+0.015) + 1.09\ln(\lambda)+1.27 \\ \times\ln(\theta+0.0001)+9.7 \quad (3GHz \le f \le 10GHz) \\ \sigma^0_{HH} - 1.73\ln(h_a+1.015)+3.67\ln(\lambda)+2.46 \\ \times\ln(\theta+0.0001)+22.2 \quad (f \le 3GHz) \end{cases} \tag{10}$$

When the transmission frequency of the radar varies from 10GHz to 100GHz,

$$\sigma^0_{HH} = 10\log(5.78\times10^{-6}\lambda\theta^{0.547}F_aF_uF_w) \tag{11}$$

$$\sigma^0_{VV} = \sigma^0_{HH} - 1.38\ln(h_a)+3.43\ln(\lambda)+1.31\ln(\theta)+18.55 \tag{12}$$

wherein, σ^0_{HH} and σ^0_{VV} stand for scattering coefficients respectively when HH and VV are taken as polarization modes. θ means scour angle. λ refers to the wavelength of the radar. h_a indicates the mean wave height of sea surface. F_w, F_u, and F_a represent adjustment factors.

In this paper, we extract the two-dimensional simulation spectrum of different wind speeds in the fixed wind zone and 320° direction along the spectral direction of the semi-empirical model, and then calculate the backscattering coefficient based on the two-scale method. The sampling point of the wind extraction area is 8 points per meter, and the wind speed at 10 meters above the sea surface is consistent with the wind speed when simulating the random rough two-dimensional sea surface. Substituting the simplified formulas (11) and (12) into equation (6), calculate the scattering coefficients of VV and HH in different polarization modes, and plot the results in the same dimension along the x and y directions. Since $\rho(x(\theta), y(\theta))$ is the surface power spectrum, the two-dimensional random phase of the correlation function $\sigma^2_{small} = \int_{K_S}^{+\infty}\int_0^{2\pi} S(K,\Theta)dkd\Theta$ of the corresponding rough surface is converted into a two-dimensional random phase quadrant, so that it is distributed between $-\pi$ and π. This is consistent with the range of parameter distribution in the previous sea surface simulation experiment, so as to meet the requirements of the comparative study of scattering results. Besides, the spatial wave number $K = K_B = 2k_i sin\theta_i$ satisfying the Bragg scattering condition should also be contained in the small-scale portion of the rough surface. Under the condition of X-band incident frequency, the fitting results are as follows:

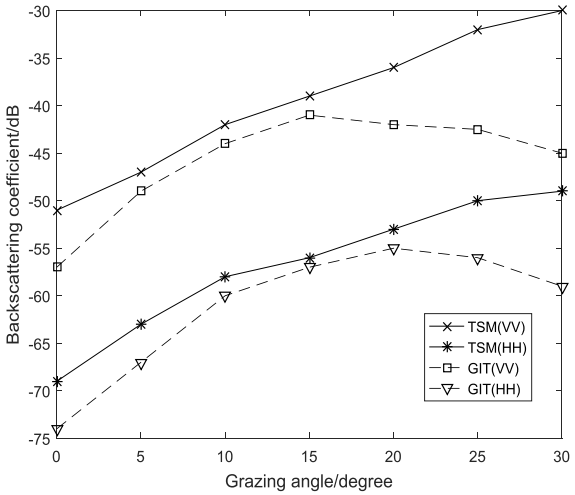

FIGURE 5. Contrast experiment of scattering coefficient between TSM and GIT models under the condition of different grazing angles.

As shown in the GIT model of Fig.5, the fitting degree gets better with the increase of grazing angle, and the fitting goodness under the HH polarization mode is higher than that under the VV polarization mode when the grazing angle is less than or equal to 15°. The fitting effect becomes worse with the increase of grazing angle when the grazing angle is greater than 15°. HH and VV polarizations are very poor in fitting effect under extremely low and high sea conditions.

Structurally similar to the GIT model, HYB and TSC models take into account the effects of atmospheric duct which are functions of grazing angle, radar wavelength, Douglas sea state, polarization mode, wind direction and beam angle (azimuth angle). The scattering rate experimental results of 1 to 5 sea state, 0.1° grazing angle, vertical polarization, and headwind (azimuth angle of 0°) are introduced as reference values in the HYB model to calculate scattering coefficient. The HYB model is defined as follows:

$$\sigma^0 = \sigma^0(ref) + K_g + K_s + K_p + K_d \tag{13}$$

wherein, $\sigma^0(ref)$ stands for the reference value for the scattering rate of 0.1° grazing angle, level 5 sea condition, vertical polarization and headwind. K_p, K_s, K_g and K_d refer to grazing angle, polarization mode, sea condition and azimuth correction factors respectively.

During the experiment, it is found that when the positive power factor $\sigma_{ref} = 2.7$, the scale factor b=1/a=1.022, the fractal dimension D_f and $M_f = K_f = 380$ in the model, the scattering coefficient of the improved Wen's spectrum of the TSM method does not only contain the positive power regular part, but also Contains a negative power law part. At the same time, it can well match the initial wave roughness distribution characteristics of the random phase distribution. Substituting the simplified formulas (13) and $k_i\sigma_{small}cos\theta_i \le 1$, $K_S < K_B = 2k_i sin\theta_i$ into equation (6), we can calculate the scattering coefficients of VV and HH in different polarization modes, and plot the results in the same dimension

along the x and y directions. Besides, the spatial wave number $K = K_B = 2k_i sin\theta_i$ satisfying the Bragg scattering condition should also be contained in the small-scale portion of the rough surface. In the actual calculation process, we extract the two-dimensional simulation spectrum of different wind speeds in the fixed wind zone and 320° direction along the spectral direction of the semi-empirical model. Under the condition of X-band incident frequency, the fitting results are as follows (Fig.6):

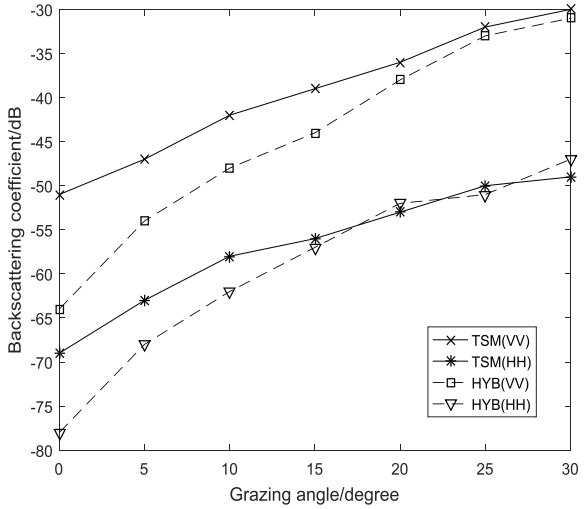

FIGURE 6. Contrast experiment of scattering coefficient between TSM and HYB models under the condition of different grazing angles.

In the TSC model, sea conditions are used for calculating effective wind speed and wave height which can also be inputted independently. The TSC model is defined as follows:

$$\sigma^0_{\mathrm{HH}} = 10\log\left(\frac{1.7\times10^{-5}\theta^{0.5}\mathrm{G_aG_uG_w}}{(\lambda+0.05)^{1.8}}\right) \tag{14}$$

$$\sigma^0_{\mathrm{VV}} = \begin{cases} \sigma^0_{\mathrm{HH}} - 1.73\ln(2.507\sigma_z+0.05)+3.76\ln(\lambda)+2.46 \\ \quad \times\ln(\sin\theta+0.0001)+19.8 \quad (f<2GHz) \\ \sigma^0_{\mathrm{HH}} - 1.05\ln(2.507\sigma_z+0.05)+1.09\ln(\lambda)+1.27 \\ \quad \times\ln(\sin\theta+0.0001)+9.65 \quad (f\le 2GHz) \end{cases} \tag{15}$$

wherein, θ stands for grazing angle. λ refers to the wavelength of radar. σ_z means the standard deviation of the sea surface's wave height. G_a, G_u and G_w represent minor grazing angle factor, wind speed factor and wind direction factor respectively.

Substituting the simplified formulas (14) and (15) into equation (6), we can calculate the scattering coefficients of VV and HH in different polarization modes, and plot the results in the same dimension along the x and y directions. Certainly, the precondition is also the satisfaction of the first-order surrounding approximation. Besides, the spatial wave number $K = K_B = 2k_i sin\theta_i$ satisfying the Bragg scattering condition should also be contained in the small-scale portion of the rough surface. Under the condition of X-band incident frequency, the fitting results are as follows (Fig.7):

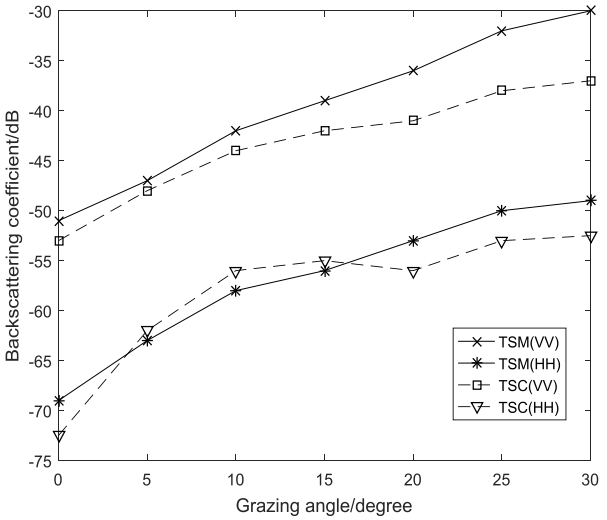

FIGURE 7. Contrast experiment of scattering coefficient between TSM and TSC models under the condition of different grazing angles.

As a backscatter coefficient model proposed by Vilhelm and Rashmi in 2009, the NRL model is only applicable to the case where wind direction and beam angle are 90° (crosswind) compared with the above three models. The NRL model [8] improved by Vilhelm and Rashmi in 2012 is defined as follows:

$$\sigma^0_{\mathrm{H,V}} = \mathrm{c}_1 + \mathrm{c}_2\cdot\log_{10}(\sin\theta) + \frac{(27.5+\mathrm{c}_3\cdot\alpha)\cdot\log_{10}(f)}{1+0.95\cdot\alpha} + \mathrm{c}_4\cdot(1+\mathrm{s})^{\frac{1}{2+0.085\cdot\alpha+0.033\cdot\mathrm{s}}} + \mathrm{c}_5\cdot\alpha^2 \tag{16}$$

wherein, θ refers to grazing angle. s represents Douglas sea level. f stands for radar frequency. $c_1 \sim c_5$ means fixed reference value.

Most semi-empirical sea clutter models are only suitable for small or medium-scale conditions of $\log_{10}(\sin\theta)$. If $\log_{10}(\sin\theta) \ge 1.25$, the extremum approximation of the right part of the above equation is negligible, because the first term in the formula already contains a large enough growth factor to compensate for the exponential decay factor. Therefore, for the big $\log_{10}(f)$, only the first item in the above formula is retained. Substituting the simplified formulas (16) into equation (6), we can calculate the scattering coefficients of VV and HH in different polarization modes. When the lateral wind is 90°, the fitting result of incident frequency under the condition of X-band incident frequency is as follows (Fig.8):

The above experimental results are analyzed to reach the following conclusions:

A. In the backscatter coefficient fitting experiment between TSM and GIT models, the fitting effect is poor at extremely low and high grazing angles, and low sea conditions and grazing angle show poor fitting effect. The fitting effect is the worst when the dividing line is 15°. Therefore, the GIT model is suitable for the simulation of medium or high sea conditions with a grazing angle of 1° to 15°.

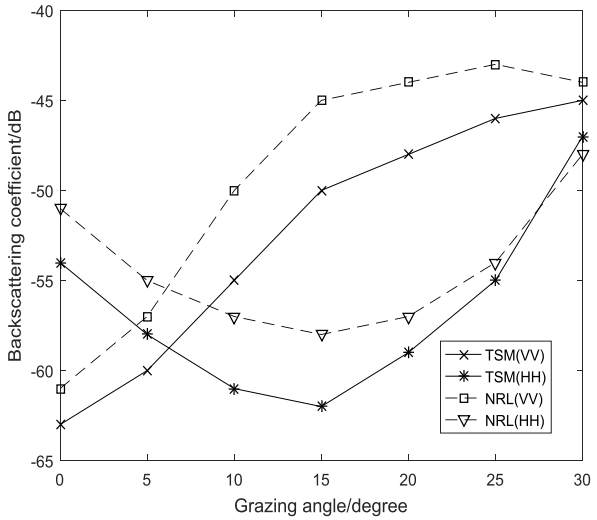

FIGURE 8. Contrast experiment of scattering coefficient between TSM and NRL models under the condition of different crosswind and grazing angles.

B. In the backscatter coefficient fitting experiment between TSM and HYB models, the HYB model is significantly better than the GIT model in fitting effect, whose goodness of fit sees an increase with the increase of grazing angle. However, the fitting effect sees no obvious change with the change of sea conditions, polarization and other factors, showing relatively poor compliance with low sea conditions and grazing angle.

C. In the backscatter coefficient fitting experiment between TSM and TSC models, the fitting characteristics of the TSC model are similar to those of the HYB model. The goodness of fit is not significantly affected by the changes in the sea state and polarization mode. The difference is that the fitting effect sees a gradual deterioration with the increase of grazing angle. On the whole, the TSC model is also better than the GIT model. Showing a good fitting effect when the grazing angle is less than or equal to 15°, the TSC model is not suitable for simulation in the case of a large grazing angle.

D. In the backscatter coefficient fitting experiment between the TSM model and the improved NRL model, the improved NRL model fits better with the measured data under various sea conditions, middle and low grazing angles and different polarization modes. However, the improved NRL model is only suitable for the case where the angle between the wind direction and the beam is 90°. Therefore, it can be first considered for the simulation of the sea surface in the case of crosswind.

IV. SUMMARY AND OUTLOOK

According to the above experiment, sea surface roughness and backscattering coefficient become larger physically due to the resonance of the sea surface resulting from the increase of sea surface roughness when the sea level increases or the wind speed becomes larger. The number of wavelength waves sees an increase, indirectly increasing the Bragg scattering of the sea surface.

In the theoretical calculation of electromagnetic scattering of improved Wen's spectrum, the experimental data under low sea conditions is greatly similar to the measured data, showing consistency with the adaptability of Wen's spectrum to the under-developed waves in China's offshore waters. In comparison with the measured data, the two-scale model with higher accuracy in the calculation of sea surface backscattering coefficient is inseparable from the two-scale method fully considering the difference of scattering mechanisms between large-scale gravity waves and small-scale tension waves.

In VV and HH polarization modes, the backscattering coefficient becomes larger with the increase of incident frequency, which is theoretically because the Bragg scattering is the main component of radar echo in the case of a relatively small grazing angle. When the sea state level is 3 and the incident frequency is L-band, the backscattering coefficient becomes larger with the increase of grazing angle within a certain range under VV and HH polarization modes.

In summary, the two-dimensional random rough sea surface simulated by the Monte Carlo method through a combination of improved Wen's power spectrum and Donelan's direction function shows consistency with the natural variation of the actual sea surface affected by the external environment (wind speed and area), whose changing characteristics are in line with physical ocean meaning. On this basis, the sea surface backscattering coefficient calculated by the two-scale method also shows similarity with the experimental data of the semi-empirical model of sea clutter. The experimental results indicate the relationship between the electromagnetic scattering coefficient of the two-dimensional sea surface simulated by improved Wen's spectrum, grazing angle, sea level and incident frequency. Through verification, the electromagnetic scattering characteristics of the two-dimensional rough sea surface of improved Wen's spectrum accords with the general physical meaning, which is of certain practical significance to study the scattering characteristics of the underdeveloped sea surface in China's offshore waters. The above conclusions provide a reference direction for future research in this field, but there are still some shortcomings. The above experiments fail to completely study the influence of sea level and incident frequency on the backscattering coefficient in the case of a great change in grazing angle. Moreover, it is temporarily impossible to study the relationship between incident azimuth and backscatter coefficient due to the lack of experimental data.

REFERENCES

[1] V. Fabbro *et al.*, "Measurements of sea clutter at low grazing angle in mediterranean coastal environment," *IEEE Trans. Geosci. Remote Sensing.*, vol. 55, no. 11, pp. 6379–6389, Nov. 2017.

[2] H. Lu, Y. Li, L. Zhang, and S. Serikawa, "Contrast enhancement for images in turbid water," *J. Opt. Soc. Amer. A, Opt. Image Sci.*, vol. 32, no. 5, pp. 886–893, 2015.

[3] N. Wang, J. Yu, B. Yang, H. Zheng, and B. Zheng, "Vision-based *in situ* monitoring of plankton size spectra via a convolutional neural network," *IEEE J. Ocean. Eng.*, to be published.

[4] H. Lu *et al.*, "CONet: A cognitive ocean network," *IEEE Wireless Commun.*, to be published.

[5] T. Wang and C. Tong, "An improved facet-based TSM for electromagnetic scattering from ocean surface," *IEEE Geosci. Remote Sens. Lett.*, vol. 15, no. 5, pp. 644–648, May 2018.
[6] G. Pan and J. T. Johnson, "A numerical method for studying modulation effects in radar observations of the sea surface," *IEEE Trans. Geosci. Remote Sens.*, vol. 46, no. 11, pp. 11803–11824, Nov. 2008.
[7] Y. Y. Hua, *Code of Hydrology for Sea Harbour*. Beijing, China: China Commun. Press, pp. 19–22, 2013.
[8] V. Gregers-Hansen and R. Mital, "An improved empirical model for radar sea clutter reflectivity," *IEEE Trans. Aerosp. Electron. Syst.*, vol. 48, no. 4, pp. 3512–3524, Oct. 2012.
[9] H. Lu, Y. Li, T. Uemura, H. Kim, and S. Serikawa, "Low illumination underwater light field images reconstruction using deep convolutional neural networks," *Future Gener. Comput. Syst.*, vol. 82, pp. 142–148, May 2018.
[10] M. Sun, Z. Gu, H. Zheng, B. Zheng, and J. Watson, "Underwater wide-area layered light field for underwater detection," *IEEE Access*, vol. 6, pp. 63915–63922, 2018.
[11] Mastrogiuseppe, Hayes, Poggiali, "Radar sounding using the Cassini altimeter: Waveform modeling and Monte Carlo approach for data inversion of observations of Titan's seas," *IEEE Trans. Geosci. Remote Sens.*, vol. 54, no. 10, pp. 5646–5656, Oct. 2016.
[12] G. K. Wu, G. R. Ji, T. T. Ji, and H. X. Ren, "Study of electromagnetic scattering from two-dimensional rough sea surface based on improved Wen's spectrum," *Acta Phys. Sinica*, vol. 63, no. 13, pp. 134203-1–134203-13, Jul. 2014.
[13] Y. Y. Hua, *Code of Hydrology for Sea Harbour*. Beijing, China: China Commun. Press, 2013, pp. 169–174.
[14] M. A. Nair and V. S. Kumar, "Wave spectral shapes in the coastal waters based on measured data off Karwar on the western coast of India," *Ocean Sci.*, vol. 13, no. 3, pp. 365–378, May 2017.
[15] X. Meng, L. X. Guo, Y. W. Wei, and J. J. Sun, "An accelerated ray tracing method based on the TSM for the RCS prediction of 3-D large-scale dielectric sea surface," *IEEE Antennas Wireless Propag. Lett.*, vol. 14, pp. 233–236, 2015.
[16] Y. Wang *et al.*, "An imaging-inspired no-reference underwater color image quality assessment metric," *Comput. Elect. Eng.*, vol. 70, pp. 904–913, Aug. 2017.
[17] W. Geng-Kun, S. Jin-Bao, and F. Wei, "Electromagnetic scattering characteristics analysis of freak waves and characteristics identification," *Acta Phys. Sinica*, vol. 66, no. 13, pp. 134302-1–134302-10, Jul. 2017.

GENGKUN WU received the B.E. degree from the College of Computer Science and Engineering, Shandong University of Science and Technology, China, in 2010, and the Ph.D. degree from the School of Computer Science and Technology, Ocean University of China, in 2015. He was a Postdoctoral Researcher with Zhejiang University, from 2015 to 2017. He is currently a Lecturer with the College of Computer Science and Engineering, Shandong University of Science and Technology. His research interests include computer simulation, modeling, and optimization, ocean wave modeling and rendering, and calculation of surface electromagnetic scattering coefficient.

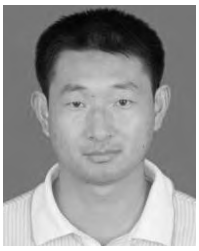

JIANCONG FAN received the B.S., M.S., and Ph.D. degrees from the College of Computer Science and Engineering, Shandong University of Science and Technology, China, in 2000, 2003, and 2010, respectively. He is currently a Professor with the Shandong University of Science and Technology, Qingdao, China. His research interests include data mining and machine learning, intelligent information processing, computer simulation, modeling, and optimization, and ocean wave modeling and rendering.

FUXIN ZHANG received the B.S. and M.S. degrees from the College of Computer Science and Engineering, Shandong University of Science and Technology, China, in 2006 and 2010, respectively, and the Ph.D. degree in Technology, China, in 2016. He is currently a Lecturer with the College of Computer Science and Engineering, Shandong University of Science and Technology. His research interests include computer simulation, modeling, and optimization, vehicular networking, cooperative vehicle safety systems, and wireless resource allocation.

TING WANG received the master's and Ph.D. degrees in computer application technologies from the Ocean University of China, Qingdao, China. She is currently a Lecturer of computer science with the Shandong University of Science and Technology, Qingdao. Her main research interests include image processing, facial recognition, and machine learning. She is a member of the China Computer Federation.